# Feasibility study for a tonal vibration control system of a mounting bracket for automotive gearboxes

D. Magliacano, M. Viscardi, M. Ciminello, I. Dimino and A. Concilio

***Abstract***—A conceptual design of an active device able to attenuate the tonal vibrations of a mounting bracket for automotive gearboxes is addressed in this paper. A preloaded piezo stack actuator is used to counteract the unbalanced vibrations of the component by monitoring its operational deformations. Firstly, a numerical modal analysis is carried out to characterize the normal modes in the frequency range of interest. The piezo stack is simulated by a rod element and its effect is numerically characterized. The upper and lower faces of the stack are mechanically coupled with the bracket structure, whereas the active control deals with the relative displacement of two points of the bracket.

The primary disturbance was simulated by a shaker to control the vibrations in correspondence of the second bending mode (around 1.6 kHz). A 20 Hz narrow band was additionally selected as the control window. Then, this frequency range was enlarged around the resonance peak in order to optimize the control effect, till 80 Hz to investigate the resulting effects. Finally, focus is given to the structural damping by assessing its impact on the control forces and phases to cancel the deformation along the contact direction. The description of the experimental results concludes this work by generally confirming the numerical expectations.

***Keywords***—active vibration control, automotive, gearbox, piezoceramic actuators

## I. INTRODUCTION

THE reduction of interior noise through active devices has been a research topic for more than 50 years [1]. In particular, active vibration control was successfully tested in many automotive and aeronautical applications [2][3]. With reference to automotive, an intense research activity dealing with structural vibro-acoustics has been addressed in the last few years [4]-[9].

A variety of independent noise sources may impact on passengers' perceived noise in vehicles. These sources may be transmitted via structural paths, and then radiated acoustically into the cabin (structural-borne noise) or acoustically generated and propagated by airborne paths (air-borne noise). In vehicles, the structure-borne noise from gearbox system excitation acts as a major contributor to the overall interior noise level, along with tire-road and aerodynamic noise [10]. The primary goal of this activity is the development of a control system, based on a piezoceramic device, for the reduction of tones in the 5-2000 Hz range of a mounting bracket for automotive gearboxes. The control is numerically simulated and implemented using the software MSC Nastran. In particular, the studied control system is based on a piezoceramic actuator in the form of a stack which, if suitably integrated in the structure, acts on specific tones of the control range, reducing the width of the structural response due to an excitation of vibrational type [11]. Compared to [12], here it's presented an analysis of the structural behavior as a function of damping and it's described the experimental activity carried out on the bracket, which confirms the obtained numerical results.

## II. PROBLEM FORMULATION

From preliminary tests conducted on the system, it appeared that it shows an annoying whistle in third gear linked to a resonance of the bracket. Therefore, the CAD model of the bracket was generated (Fig. 1) and, downstream of the application of appropriate constraint conditions, the studies have concentrated on the said component.
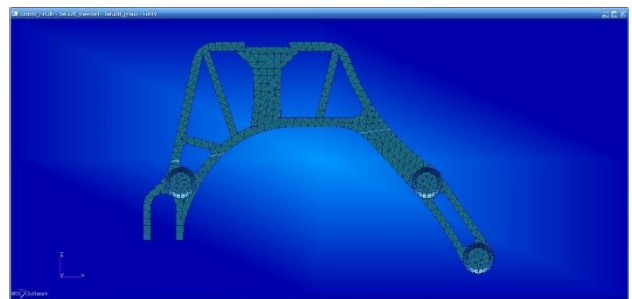


Fig. 1: Bracket CAD model

D. Magliacano is with the University of Naples Federico II, Industrial Engineering Department, Napoli (NA), ITALIA (corresponding author to provide phone: +393808147713; e-mail: darius6591@hotmail.it).

M. Viscardi is with the University of Naples Federico II, Industrial Engineering Department, Napoli (NA), ITALIA (phone: +390817683572; e-mail: maviscar@unina.it).

M. Ciminello is with the CIRA, the Italian Aerospace Research Centre, Adaptive Structures Division, Capua (CE), ITALIA (phone: +390823623535; e-mail: m.ciminello@cira.it).

I. Dimino is with the CIRA, the Italian Aerospace Research Centre, Adaptive Structures Division, Capua (CE), ITALIA (phone: +390823623308; e-mail: i.dimino@cira.it).

A. Concilio is with the CIRA, the Italian Aerospace Research Centre, Adaptive Structures Division, Capua (CE), ITALIA (e-mail: a.concilio@cira.it).

In Fig. 3-7, the shown plan is X-Z, with X that points to the right, Z points upward and Y accordingly, so as to form a left-handed triad. As already anticipated, the hypothesized solution involves the use of a piezoceramic stack that works to normal effort, whose characteristics are reported in Table (a); the stacks are constituted by a network of piezoceramics, connected mechanically in series and electrically in parallel, which allows the generation of a bigger force compared to piezoelectric patches.

Table (a): Geometrical and mechanical char. of the piezo stack

| Model | P-016.20 |
|---|---|
| Length [mm] | 29 |
| Diameter [mm] | 16 |
| Area [mm$^2$] | 201.06 |
| Stiffness [Kg/s$^2$] | $1.83 \times 10^8$ |
| Young modulus [N/mm$^2$] | $4.24 \times 10^7$ |
| Density [Kg/mm$^3$] | $7.8 \times 10^{-6}$ |
| Blocking force [N] | 5500 |
| Maximum displacement [μm] | 30 |
| Maximum supply voltage [V] | 1000 |

The graph in Fig. 2 was obtained by the formula:

$$F = F_b - Ks \qquad (1)$$

In particular, by applying the boundary condition the piezo-ceramic stiffness may be computed:

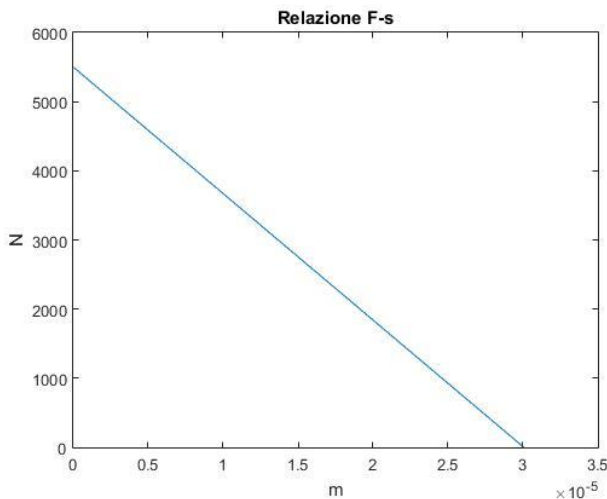$$F = 0, s = s_{max} \rightarrow K = \frac{F_b}{s_{max}} \qquad (2)$$



Fig. 2: Piezo stack: strength – displacement. Graph.

*A. Modal analysis*

Initially, it was conducted a numerical modal analysis without the piezoceramic stack, which detected two vibration modes in the 5-2000 Hz range; its results are shown, in terms of displacements and of strain energy, hereinafter in Fig. 4 and 6. Note that, since the first mode of vibration is of flexural type and is out of the plane of the bracket, the numerical control

through the use of a piezoceramic stack has been developed only in the vicinity of the second mode of vibration, which is instead in the flexional plane of the bracket . Subsequently, it was simulated the piezoceramic stack as a ROD element, with the axis tilted 14° = 0.2443 rad compared with Z axis (Fig. 3). The introduction of this additional item in the structure constitutes a reason of variation of the modal frequencies, whose general expression is:

$$\omega_N = \sqrt{\frac{K}{m}} \qquad (3)$$

Downstream of a new modal analysis, that this time takes into account the (passive) presence of the piezoceramic stack, the new modes are reported in Fig. 5 and 7, in terms of displacements and strain energy. Considering Formula (3) and the results reported in Table (b), it is possible to deduce that the introduction of the said element in the system brings a greater contribution of mass than stiffness. Note that a cylindrical device embedded within the structure and acting as a strut (as the used piezo stack), does control relative (strains) and not absolute displacements and the associated time derivatives. In fact, it arises internal forces, equivalent to zero, that cannot induce any kind of absolute movement to the structural system.

Table (b): Modal frequencies with and without the ROD element

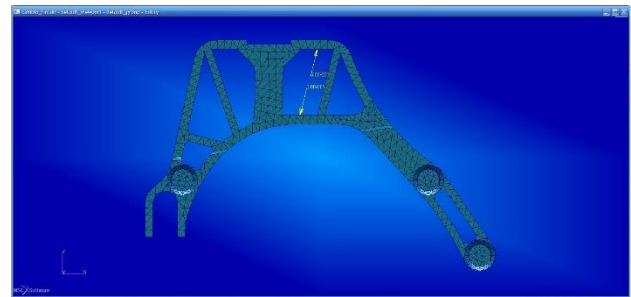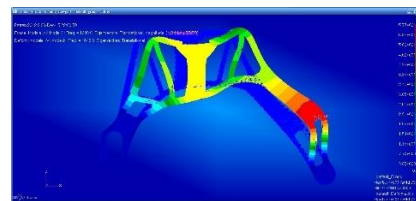| | Mode I | Mode II |
|---|---|---|
| Without ROD | 961.25 Hz | 1648.8 Hz |
| With ROD | 872.15 Hz | 1599.4 Hz |



Fig. 3: Piezo Stack Actuation direction



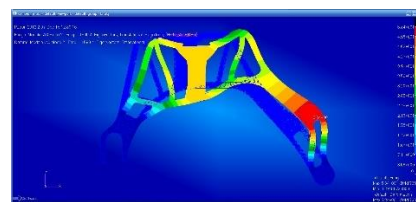Fig. 4: Displacements (without ROD) – mode 2



Fig. 5: Displacements (with ROD) – mode 2

Fig. 6: Strain energy (without ROD) – mode 2



Fig. 7: Strain energy (with ROD) – mode 2

### B. Direct and modal FRF approaches

In order to implement the control system, some FRFs in various configurations have been conducted; the MSC Nastran software offers the possibility to perform frequency response analysis using a direct or a modal technique. The latter, in particular, intrinsically constitutes an approximation of the first one, but offers considerable advantages in terms of computational time. It was therefore conducted a preliminary comparison between the two techniques. The structure was excited with an acceleration along Z equal to 1 g, applied in the left and in the lower right corner bolts, while the response was detected in terms of acceleration in a particular point of the structure (Fig. 8). As shown in Table (c), the difference between the obtained values is definitely negligible.
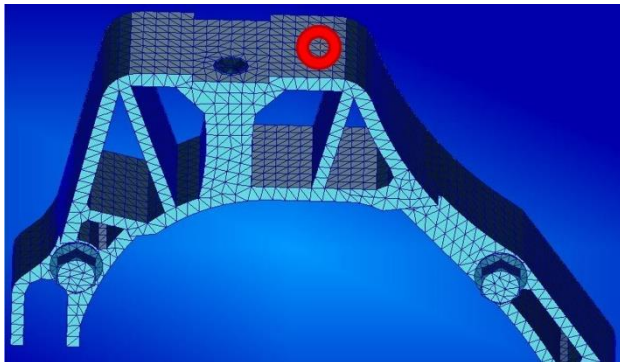


Fig. 8: Control point for the FRF comparison

Table (c): Comparison between direct and modal FRF results

|  | X [mm/s$^2$] | Y [mm/s$^2$] | Z [mm/s$^2$] |
|---|---|---|---|
| Direct | 3.8905*10$^3$ | 1.8245*10$^3$ | 6.8606*10$^3$ |
| Modal | 3.8906*10$^3$ | 1.8247*10$^3$ | 6.8601*10$^3$ |

### C. Control system implementation

The primary excitation that simulates the effect of a shaker, equal to 1 g, directed along Z and applied in correspondence of the left and the lower right bolts, is modeled in frequency as a white noise.

In order to control the deformation in the vicinity of the second mode of vibration, it is opted to implement the control at 1599.4 Hz, introducing a 1% value of damping. For this specific frequency, the phase is calculated to optimize the control action by using the formula:

$$\text{Control phase [deg]} = 180 - (B2 - B1) \qquad (4)$$

Where:
- B1 is the phase of the excitation device – sensor FRF;
- B2 is the phase of the control device – sensor FRF.

In particular, the tonal response is calculated in terms of deformation between two points located on the two opposite faces of the piezoceramic, first only due to the excitation of the shaker (a = 1 g, φ = 0°) and then solely due to the effect of the stack (F = 1 N, φ = 0°). Downstream of the reasoning set out above, two key numbers regarding the piezoceramic stack have been calculated:

- The module of the control force to be applied in order to completely cancel the deformation at a specific frequency, equal to 1.629 N; alternatively, the application of a 1 N force produces the remarkable result of attenuating the uncontrolled response by 70% (in other words, 10.5 dB).
- The optimum phase of the control force is reported in Table (d).

Table (d): Piezoceramic stack control phase

| Shaker response phase | 256.36° |
|---|---|
| Stack response phase | 354.40° |
| Control phase | 81.96° |

### III. RESULTS

Initially, as shown in Fig. 9 and 12, the range of frequencies in which to study the effect of the control was chosen equal to 20 Hz (1590 Hz - 1610 Hz); within that range, the control action has constant amplitude and phase, chosen to optimize the specific resonance conditions at 1599.4 Hz. Subsequently, it was extended the frequency range of application of the control (in a differentiated manner for F = 1 N and F = 1.629 N), in order to best control the resonance band, without varying amplitude and phase of the control force. The results of this operation are visible in Fig. 10 and 13. By further extending the control frequency range (1560 Hz - 1640 Hz, Fig. 11 and 14), as expected, an unwanted effect is produced, since doing so a disturbance (for effect of the piezoceramic stack) it's introduced at the frequencies to which the external excitation (which was modeled on the control action) is negligible compared to the effect of the control itself.

In conclusion, the optimal frequency ranges, in which the control should be extended, are:

- F = 1 N → 1576 Hz - 1624 Hz
- F = 1.629 N → 1582 Hz - 1615 Hz

The result plots are shown, expressed both in linear and logarithmic scale; the blue line shows the uncontrolled response, the red one is the control using F = 1 N and lastly the yellow one corresponds to the controlled response with F = 1.629 N.
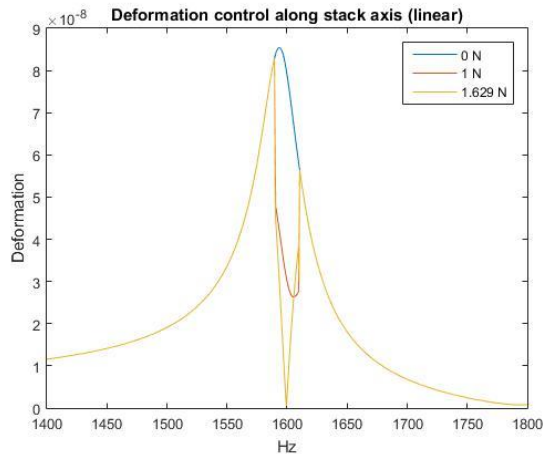


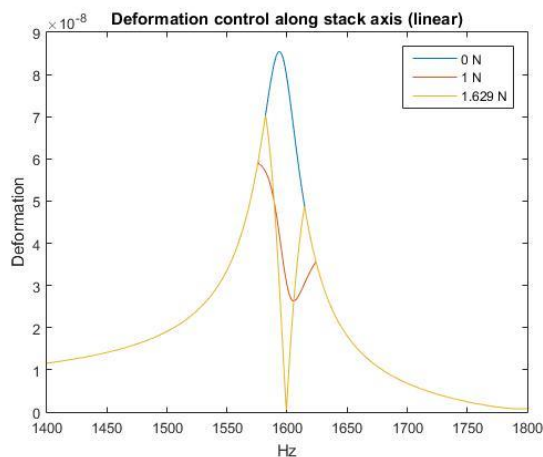Fig. 9: Control on a 20 Hz range, linear graph



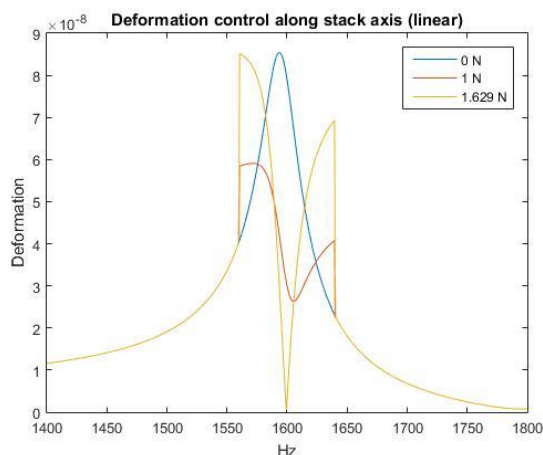Fig. 10: Optimal control, linear graph



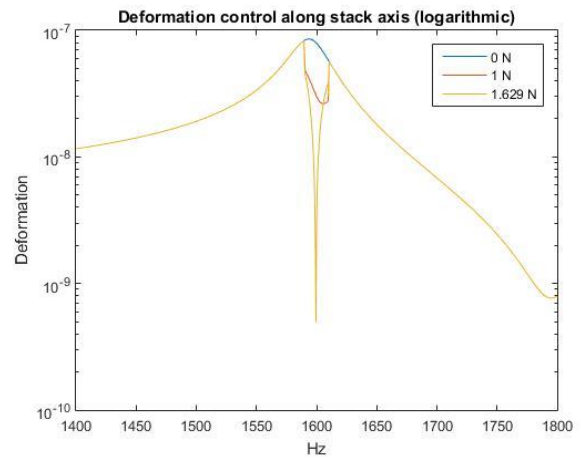Fig. 11: Control on an 80 Hz range, linear graph
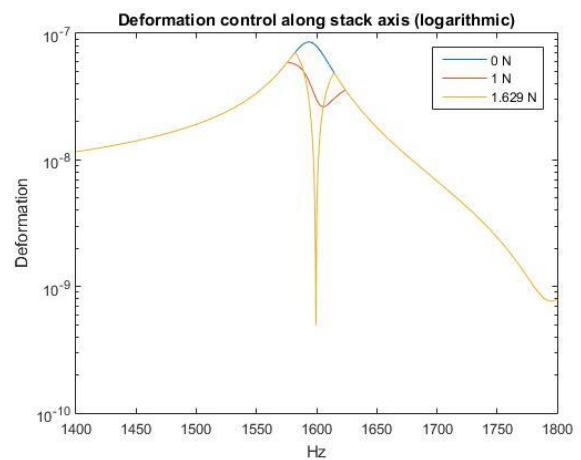


Fig. 12: Control on a 20 Hz range, logarithmic graph
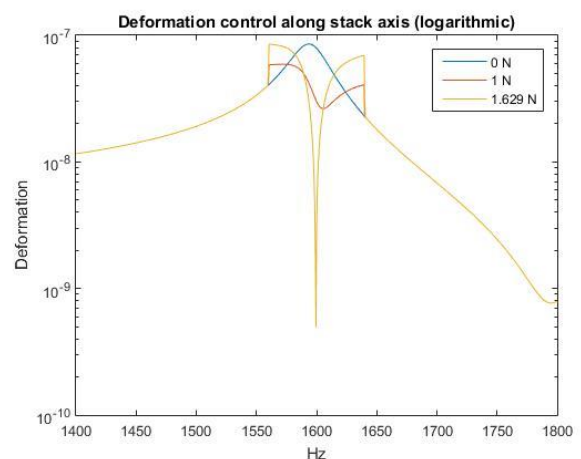


Fig. 13: Optimal control, logarithmic graph



Fig. 14: Control on an 80 Hz range, logarithmic graph

## IV. DAMPING ANALYSIS

### A. Stability study

The analysis presented so far has been conducted for a value of the structural damping equal to 1%. Here a sensitivity study is reported as a function of the structural damping in the range between 1% and 10%, centered at the second vibration mode, the root locus procedure produces a graph of where the poles of

the system are for all values of the gain K (in this case, the damping value). Real and imaginary parts of complex eigenvalues respectively represent:

- Real part = $2\zeta\omega_n$
- Imaginary part = $\omega_n^2\sqrt{1-\zeta^2} = \omega_d$

With:

- $\zeta$ = damping coefficient;
- $\omega n$ = natural frequency;
- $\omega d$ = damped frequency.

The plane (in the s-domain) may be divided into the following areas:

- A stable region → real part < 0;
- A marginally stable region → real part = 0;
- An unstable region → real part > 0.

Furthermore, an imaginary part non-null indicates the presence of oscillations in the response. When any or all of the roots of are in the unstable region, the system is unstable. When any of the roots are in the marginally stable region, the system is marginally stable (oscillatory). When all of the roots of are in the stable region, then the system is stable.

It is important to note that a control system that does produce a stable action for a certain gain K1 may become unstable for a gain K2. Some systems may have poles that cross over from stable to unstable multiple times, giving multiple gain values for which the system is unstable. In this case, the Fig. 15 shows that, in the chosen range of damping, the response of the structure is always oscillatory (as expected) and stable. In fact, increasing the structural damping from 1% to 10%, the stiffness and other properties aren't changed. An unstable behavior, instead, could happen for not collocated or partially collocated system gains, which generate not-symmetric and not-positive definite matrices.
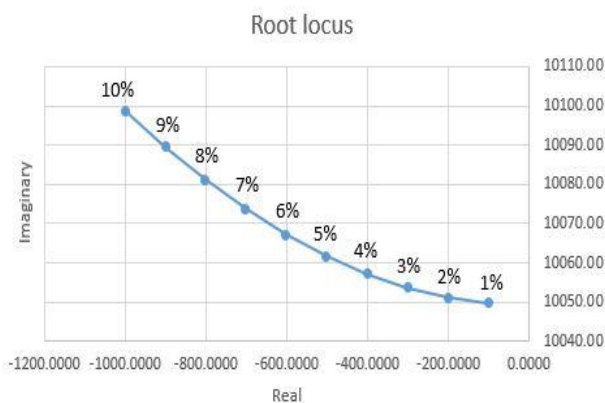


Fig. 15: Complex eigenvalues as function of the str. Damping

### B. Results for variable structural damping

Considering a structural damping range between 1% and 10%, here are reported the values of the control phases and the force magnitudes, generated by the piezo stack in order to cancel the deformation along the contact direction at the second mode. Within MSC Nastran, for each unit increase of the structural damping, the following procedure is operated:

- Calculation of the structural response phase, due to the shaker;
- Calculation the structural response phase, due to the piezo stack;
- Calculation of the optimal control phase by the previous formula;
- Calculation of the deformation magnitude at the observation point, due to the shaker;
- Calculation of the deformation magnitude due a unit force, by the stack;
- Calculation of the necessary stack axial force, to cancel the strain along its direction, having assumed a linear behavior of the examined structure.

Table (e): Complex eigenvalues vs. structural damping

| Damping | Real | Imaginary |
|---------|---------|-----------|
| 1% | -100.49 | 10049.72 |
| 2% | -200.94 | 10051.23 |
| 3% | -301.34 | 10053.74 |
| 4% | -401.65 | 10057.25 |
| 5% | -501.84 | 10061.74 |
| 6% | -601.87 | 10067.23 |
| 7% | -701.74 | 10073.69 |
| 8% | -801.39 | 10081.12 |
| 9% | -900.82 | 10089.52 |
| 10% | -999.98 | 10098.85 |

Table (f): Shaker and stack phases vs structural damping

| Damping | Shaker phase [°] | Stack phase [°] |
|---------|------------------|-----------------|
| 1% | 256.36 | 354.39 |
| 2% | 268.13 | 355.34 |
| 3% | 274.24 | 354.95 |
| 4% | 278.66 | 354.19 |
| 5% | 282.20 | 353.28 |
| 6% | 285.12 | 352.29 |
| 7% | 287.55 | 351.27 |
| 8% | 289.56 | 350.22 |
| 9% | 291.21 | 349.16 |
| 10% | 292.54 | 348.10 |

Table (g): Shaker and stack deformations vs structural damping

| Damping | Shaker def. | Stack def. (1N) |
|---------|-------------|-----------------|
| 1% | 8.00E-08 | 3.07E-08 |
| 2% | 4.19E-08 | 7.99E-09 |
| 3% | 2.86E-08 | 2.13E-08 |
| 4% | 2.21E-08 | 2.78E-08 |
| 5% | 1.82E-08 | 3.16E-08 |
| 6% | 1.57E-08 | 3.40E-08 |
| 7% | 1.40E-08 | 3.56E-08 |
| 8% | 1.27E-08 | 3.68E-08 |
| 9% | 1.17E-08 | 3.76E-08 |
| 10% | 1.10E-08 | 3.82E-08 |

Table (h): Block force – phase & magnitude vs str. damping

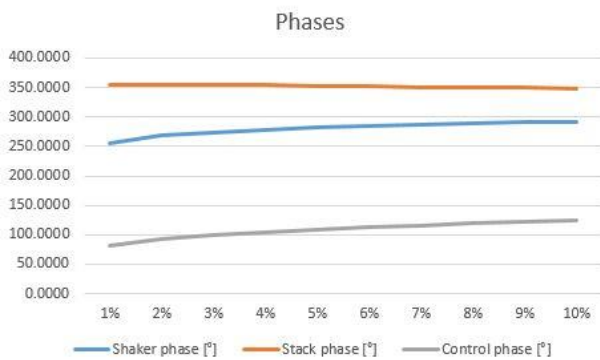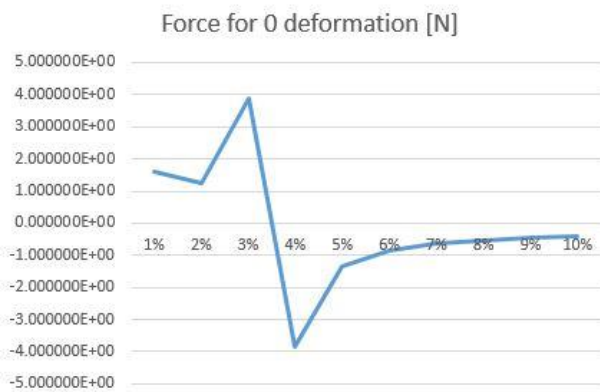| Damping | Control phase [°] | Force for null def. [N] |
|---------|-------------------|-------------------------|
| 1% | 81.96 | 1.62E+00 |
| 2% | 92.79 | 1.24E+00 |
| 3% | 99.29 | 3.90E+00 |
| 4% | 104.47 | -3.84E+00 |
| 5% | 108.92 | -1.36E+00 |
| 6% | 112.83 | -8.60E-01 |
| 7% | 116.29 | -6.46E-01 |
| 8% | 119.35 | -5.28E-01 |
| 9% | 122.05 | -4.54E-01 |
| 10% | 124.44 | -4.04E-01 |

Fig. 16: Phases as functions of critical damping

Fig. 17: Block force vs structural damping

## V. EXPERIMENTAL ACTIVITIES

As conclusion, it is shown the experimental work which was conducted on the bracket of the gearbox; in particular, the bracket was installed on the shaker of the C.I.R.A. vibro-acoustic testing laboratory through the use of two angular interfaces (Fig. 18) and two FRFs between 1300 Hz and 1800 Hz were acquired, respectively generated from the shaker (Fig. 19) and the piezoceramic stack (Fig. 20). Evidently, the resonance frequencies are different and more numerous than those identified by the numerical analysis: this can be explained by the additional presence of the two angular interfaces. The experimental resonance nearest to the numeric one is at about

1580 Hz; this made it the best candidate around which carry out experimental control tests necessary to validate the numerical model discussed.
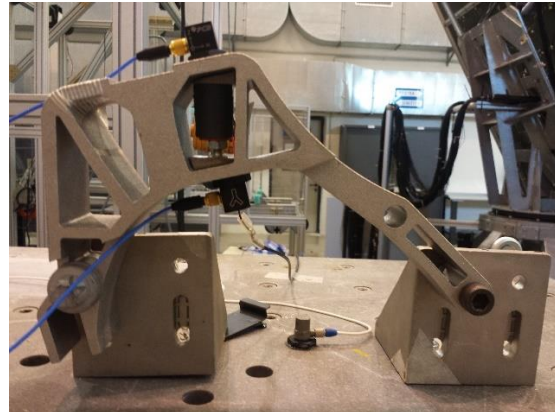
Fig. 18: Bracket with stack installed on the shaker; in the vicinity of the piezoceramic, two accelerometers are visible

At this frequency, it is recorded the response, in terms of amplitude and phase, due to an excitation equal to 1 g produced from the shaker and, subsequently, equal to 1 N produced from the piezoceramic stack. Responses were obtained from two accelerometers in terms of acceleration; since they are in the frequency domain, starting from them it is possible to trace the amplitude of displacements of the analyzed two points by the formula:

$$\Delta x = \frac{|\ddot{x}|}{\omega^2} \tag{5}$$

And, accordingly, it is possible to calculate the strain:

$$\varepsilon = \frac{\Delta x}{\text{reference distance}} \tag{6}$$

Finally, they are calculated optimal amplitude and phases for the control, following the same reasoning described in paragraph 2.C. Below there is a summary table of the results obtained during the above procedure.
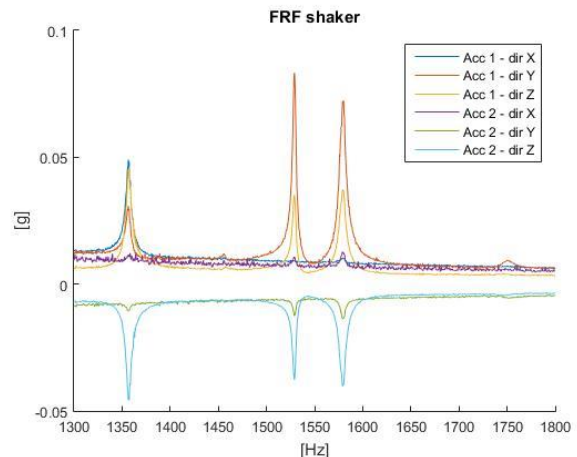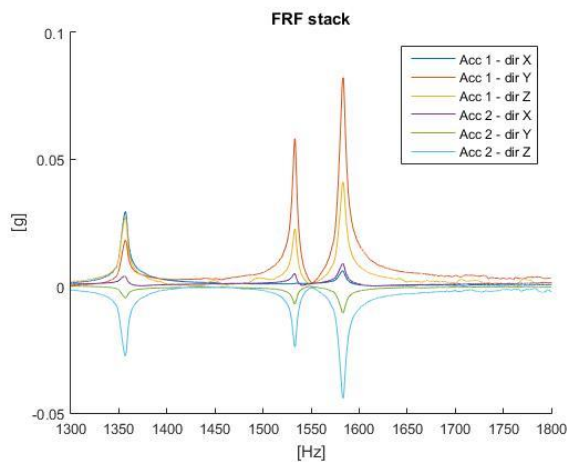
Fig. 19: FRF by the shaker action

Fig. 20: FRF by the stack action

Table (i): Summary of experimental activity results

| shaker up | sh. down | stack up | st. down | |
|-----------|----------|----------|----------|------|
| 0.037 | -0.040 | 0.028 | -0.030 | g |
| 0.363 | -0.391 | 0.275 | -0.293 | m/s$^2$ |
| 3.68E-09 | -3.97E-09 | 2.78E-09 | -2.97E-09 | m |
| 7.654E-09 | | 5.763E-09 | | m |
| 7.654E-06 | | 5.763E-06 | | mm |
| 1.644E-07 | | 1.237E-07 | | def. |
| 1.3301 | | | | N |

It can be noted that, compared to this result, the numerical one has a positive error of about 22%. The frequency range of application of the control was extended (in a differentiated manner for F = 1 N and F = 1.3301 N), in order to best control the "bell" of the resonance peak, without varying amplitude and phase of the control force; the results of this operation are visible in Fig. 21. This evidence can be a measure of the stability of the system, with respect to investigated frequencies. As in the numerical analysis, by further extending the control frequency range (1560 Hz - 1600 Hz, Fig. 22), as expected, an unwanted effect is produced. In conclusion, the optimal frequency ranges in which to extend the control are:

- F = 1 N → 1572 Hz - 1586 Hz
- F = 1.3301 N → 1574 Hz - 1584 Hz

It can be noted that, as already shown in the numerical results, the optimum range of application of the control predictably shrinks with increasing applied force. The result plots are expressed in linear scale; the blue line shows the uncontrolled response, the red one is the control using F = 1 N and lastly the yellow one corresponds to the controlled response with F = 1.3301 N. The application of a unit force, in any case, produces a remarkable result, breaking down the uncontrolled response of about 75% (in other words, of about -12 dB); this is 5% better compared to the numerical result. Indeed, the control should have variable amplitude and phase as functions of frequency. In other words, for different frequencies, the amplitude and phase values are different and so they should be recalculated: there is a vector of amplitude and phase values,

the frequency is recognized with a synchro signal and it is selected the numerical couple to best attenuate the noise).
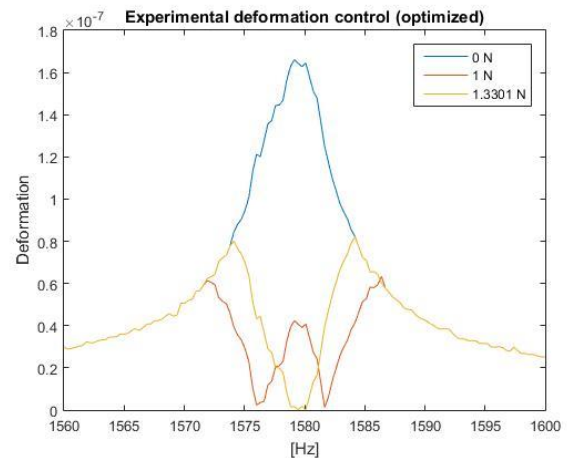

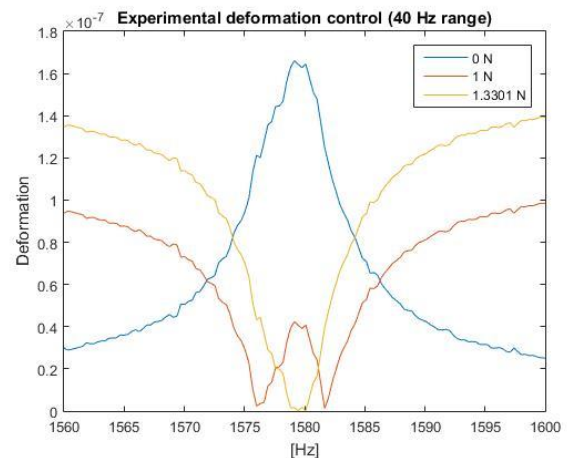Fig. 21: Experimental optimal control


Fig. 22: Experimental control on a 40 Hz range

REFERENCES

[1] K. Seto Preumont, *Active Control of Structures*. Wiley, (2008).
[2] M. Viscardi, L. Lecce, "An integrated system for active vibro-acoustic control and damage detection on a typical aeronautical structure", Paper presented at the IEEE Conference on Control Applications – Proceedings.
[3] L. Lecce, M. Viscardi, G. Zumpano, "Multifunctional system for active noise control and damage detection on a typical aeronautical structure", Proceedings of SPIE - The International Society for Optical Engineering, 4327, pp. 201-212.
[4] P. Lardeur, M. Scionti, R. Scigliano, "Verification and validation of finite element models for the vibro-acoustic behaviour of a windscreen in presence of variability", Proceedings of the ISMA 2006 congress, 2006, pp. 1951-1962.
[5] S. Turrin, M. Hanss, L. Gaul., "Fuzzy arithmetical vibration analysis of a windshield with uncertain parameters", Proceedings of the IX International Conference on Recent Advances in Structural Dynamics - RASD05, 2006.
[6] C. Fernandez, C. Soize, L. Gagliardini, "Modeling sound-insulation layers in vibroacoustic systems", Proceedings of the 1st International Conference on Uncertainty in Structural Dynamics, 2007, pp. 331-340.
[7] C. Lionnet, P. Lardeur, "A hierarchical approach to the assessment of variability of interior noise levels in passenger cars", Noise Control Engineering Journal, vol. 55, 2007, pp. 29-37.
[8] C. Lionnet, P. Lardeur, F. Vieuille, "A hierarchical approach to study the intra and intervariability of structure borne noise in vehicles", Proceedings of the ISMA 2006 congress, 2006, pp. 4175-4186.

[9]  T. Cardone, R. Dippolito, S. Donders, H. Van der Auweraer, L. P. R. De Oliveira, M. da Silva, "Robustness Assessment and Optimization of a Simpli_ed Smart Structure Model for Structural Acoustic Control", Proceedings of LSAME.08, 2008, pp. 617-628.

[10] F. Svaricek, T. Fueger, H. Karkosch, P. Marienfeld, C. Bohn, *Automotive Applications of Active Vibration Control*. University of the German Armed Forces Munich, Technical University Clausthal.

[11] S. Leleu, H. Abou-Kandil, Y. Bonnassieux, "Piezoelectric actuators and sensors location for active control of exible structures", IEEE Transactions on Instrumentation and Measurement, vol. 50, 2002.

[12] D. Magliacano, M. Ciminello, I. Dimino, M. Viscardi, A. Concilio, "Active vibration control of a mounting bracket for automotive gearboxes", International Journal of Mechanical Engineering, 2016, pp. 69-74.

**D. Magliacano** was born in 1991 and lives in Naples. He studied at the University of Naples "Federico II" and in 2013 obtained a Bachelor Degree in aerospace engineering, presenting a thesis entitled "Innovative methodologies for predictive analysis of the internal noise in rail vehicles". Then, in 2016, downstream of 4 months of internship at the Italian Aerospace Research Centre, he completed the Master Degree with a mark of 109/110, discussing the thesis "Active control of noise and vibrations in automotive".

Other papers:

- Active vibration control by piezoceramic actuators of a car floor panel (Naples, Italy: Proceedings of the ICSV23 conference, 2016)
- Active vibration control of a mounting bracket for automotive gearboxes (Naples, Italy: International Journal of Mechanical Engineering, 2016)